Available online at www.garmian.edu.krd

Passer Journal

Passer 7 (Issue 1) (2025) 70-79

Original Article

Synthesis and Characterization of (Co_3O_4-Cuo) Thin Films with Varying Mixture Ratios

Zahraa Qais Barrad Ali*[1], Nabeel Ali Bakr[1], Mahmood Mohammed Kareem[2,3]

[1]*Department of Physics, College of Science, University of Diyala, Diyala, Iraq.*

[2]*College of Education, University of Garmian, Kalar, Kurdistan Region, Iraq.*

[3]*Kifri Technical College, Garmian Polytechnic University, Kurdistan Region, Iraq.*

Received 30 December 2024; revised 4 February 2025;
accepted 10 February 2025; available online 19 February 2025

DOI: 10.24271/PSR.2025.496471.1879

ABSTRACT

This study investigates the deposition of Co_3O_4-CuO thin films with varying CuO ratios (20%, 40%, 60%, and 80%) using the chemical spray pyrolysis technique. The impact of CuO content on the structural, morphological, optical, and electrical properties of the films is systematically analyzed. X-ray diffraction (XRD) analysis reveals a polycrystalline nature with a dominant (113) orientation, and crystallite size increases with higher CuO content. Field Emission Scanning Electron Microscopy (FE-SEM) shows that CuO incorporation leads to denser, more homogeneous films with larger grain sizes. UV-Vis spectroscopy indicates a decrease in the energy band gap with increasing CuO ratio, with the best absorbance observed in the 20% Co_3O_4: 80% CuO thin film. Photoluminescence spectra suggest excitonic emission peaks in the range of 500–900 nm, with varying peak positions as CuO content changes. Hall effect measurements confirm p-type conductivity for all films, with the 80% Co_3O_4: 20% CuO film exhibiting higher electrical conductivity than the 60% Co_3O_4: 40% CuO film. These findings highlight the significance of CuO incorporation in tuning the properties of Co_3O_4 thin films, making them promising for various optoelectronic applications.

Keywords: Co_3O_4-CuO, mixing ratios, photoluminescence, metal oxide thin films, chemical spray pyrolysis.

1 Introduction

Cobalt oxide (Co_3O_4) thin films have attracted significant interest due to their potential applications in various technological fields, such as high-temperature solar selective absorbers [1], anodic electrochromic materials for smart windows [2], and negative electrodes in lithium-ion batteries [3]. Cobalt oxide exists in three distinct crystalline forms: CoO, Co_2O_3, and Co_3O_4 [4]. The unique properties of Co_3O_4 arise from its spinel crystal structure, which contains vacancies that enhance its chemical stability, making it particularly suitable for electrochemical applications [5]. Several deposition techniques have been employed to synthesize Co_3O_4 thin films, including RF magnetron sputtering, atomic layer deposition [6], chemical vapour deposition [7], Sol–gel processing [8], co-precipitation [9], pulsed laser deposition [10], chemical bath deposition [11], and spray pyrolysis [12]. Among these methods, spray pyrolysis is particularly advantageous due to its low cost, adaptability, ease of use for large deposition areas, and ability to produce nanostructured thin films [13]. The porous structure of Co_3O_4 films facilitates the intercalation and deintercalation of small ions such as H^+, Li^+, and Na^+, making it highly desirable for improving electrochromic performance. Therefore, controlling the morphology of Co_3O_4 thin films is essential for optimizing their properties. Despite its promising characteristics, Co_3O_4 thin films face limitations in conductivity and performance, especially in high-demand electrochemical systems. To address these challenges, there has been increasing interest in enhancing Co_3O_4 thin films by doping them with various materials, such as cupric oxide (CuO), a well-known p-type semiconductor, which has a band gap range of 1.2 to 1.9 eV, CuO is particularly suited for solar cell applications [14]. CuO's semiconducting properties are attributed to Cu vacancies in its monoclinic structure (C2/c space group). By combining Co_3O_4 with CuO, the resulting composite films can exhibit enhanced properties, including improved electrical conductivity, optical characteristics, and electrochemical performance. However, optimizing the composition and performance of Co_3O_4-CuO thin films remains a challenge due to the complex interplay between the properties of each material and the fabrication conditions.

This study focuses on the preparation of Co_3O_4-CuO composite thin films using the spray pyrolysis route, with varying CuO content, and investigates their structural, morphological, optical, and electrochemical properties. The selection of CuO as a dopant

* Corresponding author
E-mail address zahraaq489@gmail.com (Instructor).
Peer-reviewed under the responsibility of the University of Garmian.

is motivated by its complementary properties to Co_3O_4, aiming to improve the material's performance in energy applications. The films are characterized using X-ray diffraction (XRD) for crystallographic analysis, Field Emission Scanning Electron Microscopy (FE-SEM) for morphological studies, UV-Vis spectroscopy to assess optical properties, and Hall effect measurements to evaluate electrical conductivity. By analyzing the relationship between CuO content and the films' properties, this work seeks to develop optimized Co_3O_4-CuO thin films with enhanced performance for various technological applications.

2 Materials and methods

Co_3O_4:CuO thin films were prepared by spraying an aqueous solution of cobalt nitrate hexahydrate ($Co(NO_3)_2 \cdot 6H_2O$) and copper chloride dihydrate ($CuCl_2 \cdot 2H_2O$) from [Oxford Lab Chem, India] and [PVT LTD, India], respectively, with CuO concentrations of 20%, 40%, 60%, and 80%. The solution was prepared by dissolving the appropriate amounts of $Co(NO_3)_2 \cdot 6H_2O$ and $CuCl_2 \cdot 2H_2O$ powders in distilled water with the same molarity(M=0.25). The required weights (Wt), as in Table 1, of each material were determined using the following equation:

$$M = \frac{\text{Wt}}{\text{Mwt}} \text{x} \frac{1000}{V} \quad (1)$$

Where M represents molarity (0.25), Wt. stands for weight, V denotes volume, and Mwt refers to molecular weight.

Table 1: The appropriate weights of the raw materials.

Ratios	$Co(No_3)_2.6H_2O$	$CuCl_2.2H_2O$
80%Co_3O_4:20%CuO	5.82	0.87
60%Co_3O_4:40%CuO	4.36	1.74
40%Co_3O_4:60%CuO	2.91	2.61
20%Co_3O_4:80%CuO	1.45	3.49

To achieve a homogeneous solution, the mixture was stirred magnetically for 20 minutes and allowed to settle. The resulting solution was then sprayed onto a heated microscope glass substrate at 400°C with CuO ratios of 20%, 40%, 60%, and 80%. Thin film with good adhesion and stability were formed on the substrate surface as a result of a chemical reaction initiated by spraying. To optimize the properties of the films, they were annealed at 500°C.

Uniform spraying was crucial to achieving homogeneity. The spray duration was set to five seconds, followed by a 35-second pause between consecutive sprays durations. Critically the distance between the capillary tube and the substrate determined the uniformity of the film deposition. The optimal nozzle height was 12cm. Increasing this distance led to dispersion the atomized solution, while reducing it caused droplets to accumulate and affected film uniformity. As shown in Table 2, film thickness was observed to increase with increasing CuO content ratio.

Table 2: Thickness of Co3O4: CuO samples.

Ratios	Thickness (nm)
80%Co_3O_4:20%CuO	75
60%Co_3O_4:40%CuO	88
40%Co_3O_4:60%CuO	89
20%Co_3O_4:80%CuO	90

3 Characterization Techniques

The morphological features of the obtained films were characterized using a field emission electron microscope (FE-SEM, TESCAN MIRA3 FRENCH) with energy dispersive spectroscopy EDS, from Arya Lab. Iran. The structure and diffraction patterns of the obtained films were investigated by XRD Philips X'Pert PA, analytical instrument from Kashan University, Iran. Photoluminescence (PL) spectroscopy was measured using an Ossila instrument from UK. The optical properties were characterized using a Shimadzu UV-2600 spectrophotometer. For conductivity measurement, the Hall effect equipment Ecopia-amp 55t- South Korea by photon-center in Baghdad was applied.

4 Results and Discussion

4.1 XRD analysis

Figure 1 presents the X-ray diffraction (XRD) patterns of thin films composed of 80% Co_3O_4 mixed with 20% CuO, both before and after annealing. Initially, all observed peaks correspond to Co_3O_4, as confirmed by matching with ICDD card no. 98-002-6723. This phase exhibits a cubic crystal system, with the highest intensity peak at $2\theta = 36.467°$, indicating a dominant growth orientation along the (113) plane. The crystalline size(D) was estimated using Scherrer's equation [15].

$$D = K\lambda / \beta \cos\theta \quad (2)$$

The crystal size before annealing was 13.49 nm. After annealing, the XRD pattern was consistent with ICDD card numbers 98-002-7505 for Co_3O_4 and 98-008-7122 for CuO, which reveal ten peaks associated with Co_3O_4 planes (111), (022), (113), (004), (133), (224), (115), (044), (135), and (335), as well as three peaks corresponding to CuO planes (11-1), (111), and (004). The highest intensity peak after annealing appears at $2\theta = 37.030°$, with the (113) plane remaining the dominant growth orientation, while the crystallite size decreases to 12.87 nm because of an increase in peak broadening [16]. The shift may be due to stress/strain from the CuO mixing ratio, which lead to contraction and the observed shift to higher angles of diffraction.

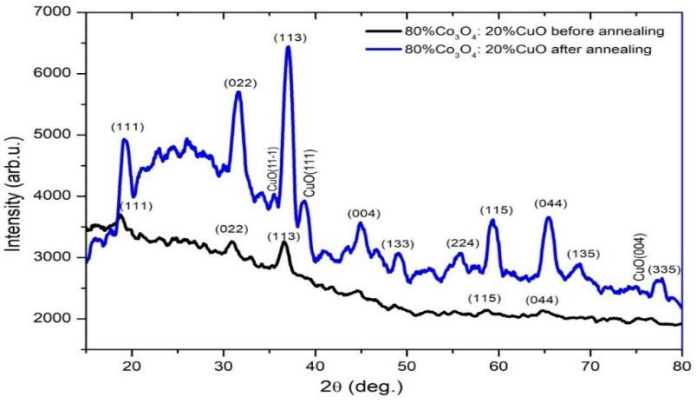

Figure 1: X-ray diffraction patterns of 80% Co3O4 mixed with 20% CuO thin film before and after the annealing.

Figure 2 shows the XRD patterns of thin films composed of 60% Co_3O_4 and 40% CuO, both in the as-deposited and annealed states. Two peaks corresponding to Co_3O_4 were identified, as verified by matching with ICDD card no. 98-002-6729. The cubic crystal system was confirmed, with the highest intensity peak at $2\theta = 36.48°$, signifying a dominant growth orientation along the (113) plane. The crystallite size before annealing was calculated to be 9.7 nm. After annealing, the XRD patterns, matched with ICDD card no. 98-002-7505 and 98-008-7122, exhibited six peaks corresponding to Co_3O_4 planes (111), (022), (113), (004), (133), and (115), and three peaks corresponding to CuO planes (11-1), (200), and (31-1). The highest intensity peak shifted to $2\theta = 37.056°$, with the (113) plane remaining the dominant growth orientation. The crystallite size after annealing increased to 14.32 nm. The intensity of CuO-related peaks in the XRD pattern increased with higher CuO content due to a greater volume fraction of CuO crystals in the mixture, resulting in stronger diffraction signals. The Scherrer equation shows that peaks corresponding to smaller crystallites are broader, whereas peaks for larger crystallites are sharper.

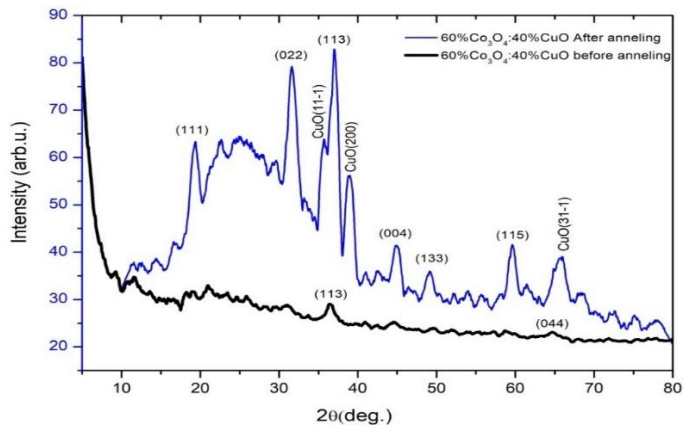

Figure 2: X-ray diffraction patterns of 60% Co_3O_4 with 40% CuO thin films, before and after the annealing.

Figure 3 displays the XRD patterns of thin films composed of 40% Co_3O_4 and 60% CuO, both before and after annealing. The diffraction pattern for the annealed film, when compared with ICDD card no. 98-002-6720, reveals two distinct peaks corresponding to Co_3O_4 at (022) and (113) planes direction, and two more peaks for CuO at (002) and (111) planes. The crystal system remains cubic and the most intense peak is at $2\theta = 35.51°$, indicating a predominant growth orientation along (002) plane. The crystallite size was determined to be 18.54 nm before annealing. After annealing, comparison with ICDD card nos. 98-002-7505 and 98-008-7122 revealed five peaks corresponding to Co_3O_4 at (022), (113), (004), (133), and (115), and four peaks for CuO at (002), (111), (02-2), and (220). The intensity of CuO-related peaks increased with higher CuO content due to a greater volume fraction of CuO crystals, strengthening the diffraction signals. The highest intensity peak shifted to $2\theta = 35.75°$, with (002) remaining the dominant growth orientation. The crystallite size after annealing was calculated as 20.36 nm. As CuO content increased, the dominant phase observed in the XRD pattern shifted from Co_3O_4 to CuO, indicating changes in phase composition and crystal orientation. The composition had a direct effect on crystallite size. As crystallite size decreased, the corresponding XRD peaks broadened, while larger crystallites produced sharper peaks.

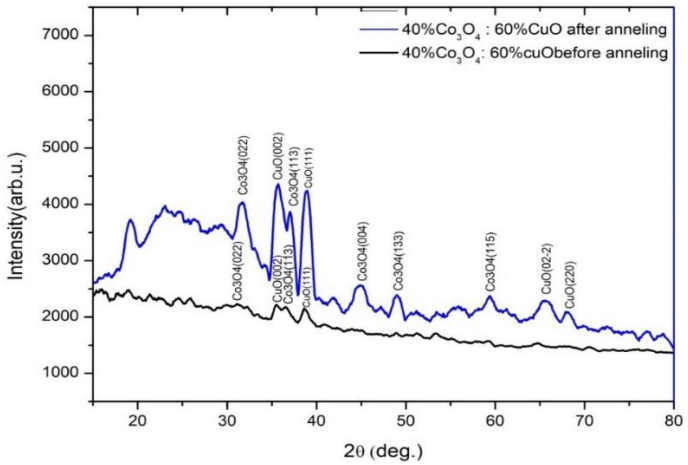

Figure 3: X-ray diffraction patterns of 40% Co_3O_4 with 60% CuO thin film before and after the annealing.

Figure 4 presents the XRD patterns of thin films composed of 20% Co_3O_4 and 80% CuO, both before and after annealing. In the annealed state, the diffraction pattern matched with ICDD card number 98-002-6720 and 98-008-7122, we observed one peak for Co_3O_4 at (113) and one for CuO at (110) plane. The cubic crystal system was confirmed, with the highest intensity peak at $2\theta = 32.49°$, indicating a dominant growth orientation along (110). The crystallite size before annealing was calculated as 10.42 nm. After annealing, the XRD pattern, was consistent with the expected pattern for ICDD card no. 98-002-7505 and 98-008-7122, revealed three peaks for Co_3O_4 at (022), (004), and (133), and eight peaks for CuO at (11-1), (200), (112), (020), (11-3), (31-1), (220), and (004). As CuO content increased, the diffraction peaks corresponding to CuO became more pronounced, while those for Co_3O_4 diminished or disappeared, indicating a shift in phase composition. The most intense peak was observed at $2\theta = 35.72°$, with the dominant growth

orientation being (11-1). Increasing CuO content altered the dominant phase in the XRD pattern from Co_3O_4 to CuO, leading to changes in crystal orientation and growth trends. After annealing, the crystallite size increased to 22.38 nm [17].

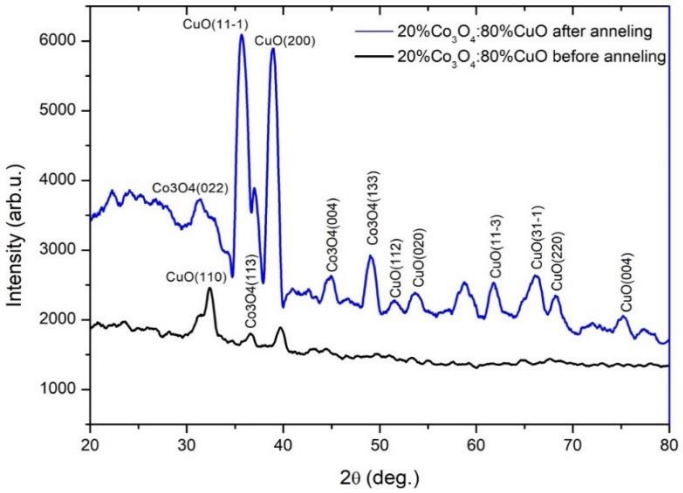

Figure 4: X-ray diffraction patterns of 20% Co_3O_4 with 80% CuO thin film before and after the annealing.

Figure 5 shows an increase in crystallite size with a higher CuO mixing ratio. The crystallite size is influenced by changes in composition. According to the Scherrer equation, peaks corresponding to smaller crystallites appear broader, while those associated with larger crystallites are sharper. As CuO content increases, the crystallite size of the dominant CuO phase may grow, leading to sharper diffraction peaks, as shown in Table 3 [18].

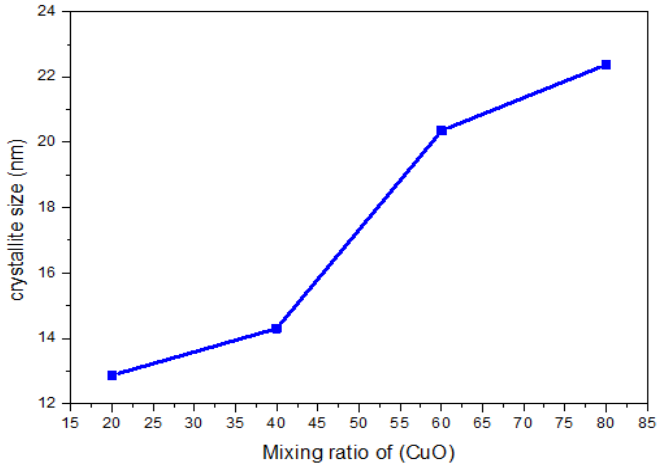

Figure 5: the relation between crystallite size and mixing ratio.

Table 3: Crystallite size of Co_3O_4: CuO samples.

Mixed ratio	Crystallite size before annealing (nm)	Crystallite size after annealing (nm)
80% Co_3O_4 : 20% CuO	13.49	12.87
60% Co_3O_4 : 40% CuO	9.7	14.32
40% Co_3O_4 : 60% CuO	18.54	20.36
20% Co_3O_4 : 80% CuO	10.42	22.38

4.2 FE-SEM Analysis of Co_3O_4: CuO Thin Films

The surface morphology of Co_3O_4: CuO thin films deposited on glass substrates via the chemical spray pyrolysis technique was examined using Field Emission Scanning Electron Microscopy (FE-SEM) after annealing. FE-SEM micrographs of the Co_3O_4: CuO films at 200KX magnification are presented in Figure 6(a–d). The surface morphology of Co_3O_4 with CuO incorporation exhibits variations, tending to become densely packed.

Figure 6(a) shows the surface morphology of an 80% Co_3O_4:20% CuO thin film, revealing a dense, smooth, and homogeneous structure with pinholes. The grains exhibit a combination of nano-cauliflower and spherical-like shapes with varying sizes, consistent with previous studies [19].

Figure 6(b) presents the FE-SEM micrograph of a 60% Co_3O_4:40% CuO thin film, showing a non-homogeneous structure with large clusters of spherical or semi-spherical grains in certain regions, indicating an irregular grain growth rate. Additionally, defects such as cracks and pinholes are visible.

Figures 6(c) and 6(d) demonstrate that increasing the CuO mixing ratio results in larger grain sizes with sharp-edged structures. The films appear denser, smoother, and more homogeneous, with a mixture of nano-cauliflower and spherical-like grains of different sizes. The particle size of the prepared samples, analyzed using ImageJ software, is summarized in Table 4, showing an increase in particle size with a higher CuO mixing ratio; as illustrated in Figure7, the histograms show the increase of the particle size up to 43.82 nm for maximum mixing ratio of CuO which is 80%, this was also can be seen clearly in figure 8, which represent the increase in particle size with increasing the content of CuO up to 80%.

Table 4: Particle size of Co3O4: CuO samples.

Co_3O_4 : CuO Samples	Particle Size (nm)
80%Co_3O_4:20%CuO	27.08
60%Co_3O_4:40%CuO	33.22
40%Co_3O_4:60%CuO	36.35
20%Co_3O_4:80%CuO	43.82

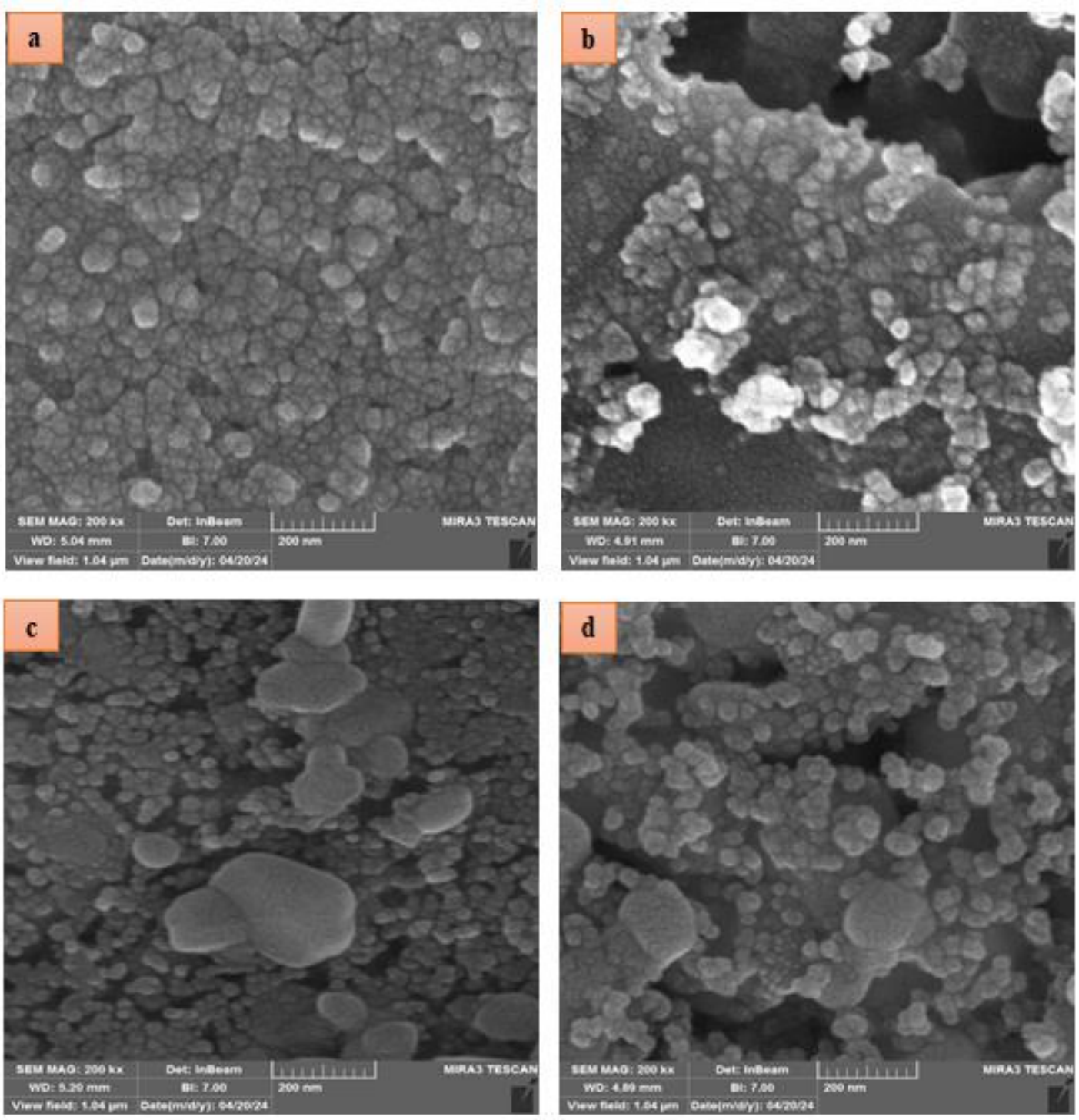

Figure 6: FE-SEM images of (a)80% Co_3O_4: 20%CuO (b) 60% Co_3O_4: 40%CuO (c) 40% Co_3O_4: 60%CuO (d) 20% Co_3O_4: 80%CuO thin film.

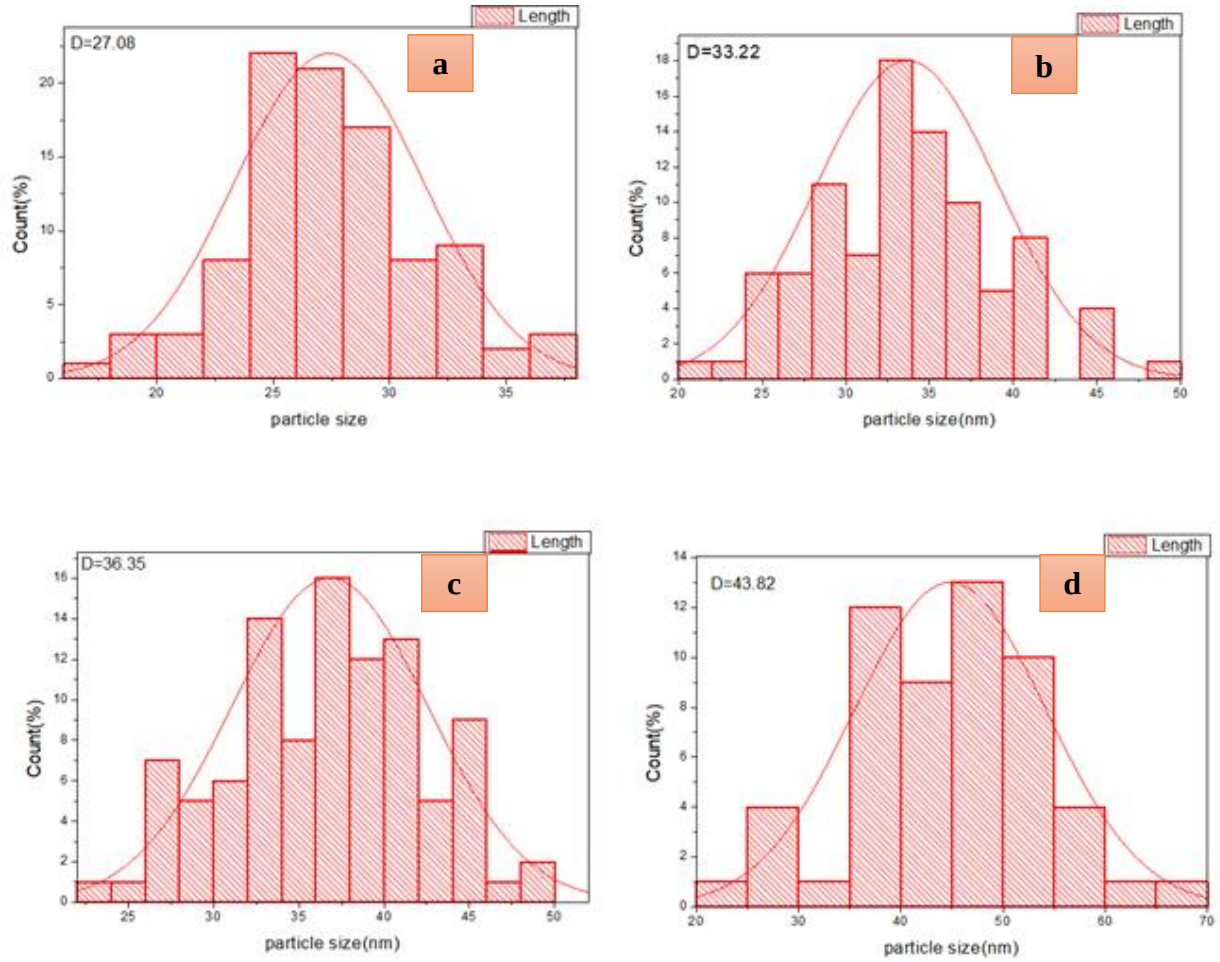

Figure 7: The Histogram of Co_3O_4 with (20%, 40%, 60% and 80%) CuO thin films.

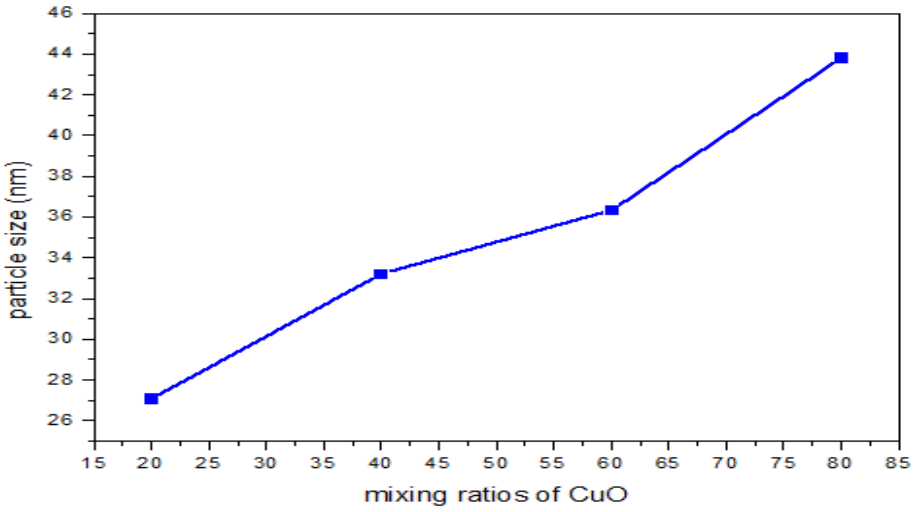

Figure 8: The relation between particle size with different mixing ratio of CuO.

Energy Dispersive Spectroscopy (EDS) spectra of Co_3O_4: CuO thin films are presented in Figure 9, with the corresponding quantitative chemical analysis listed in Table 5. The study confirms the presence of Co, O, Cu, Ca, and Cl elements. Ca is attributed to the glass substrate used during deposition, while Cl originates from $CuCl_2 \cdot 2H_2O$, which was used as the CuO precursor.

Where:

W%: Represents the weight ratio

A%: Represents the atomic weight ratio

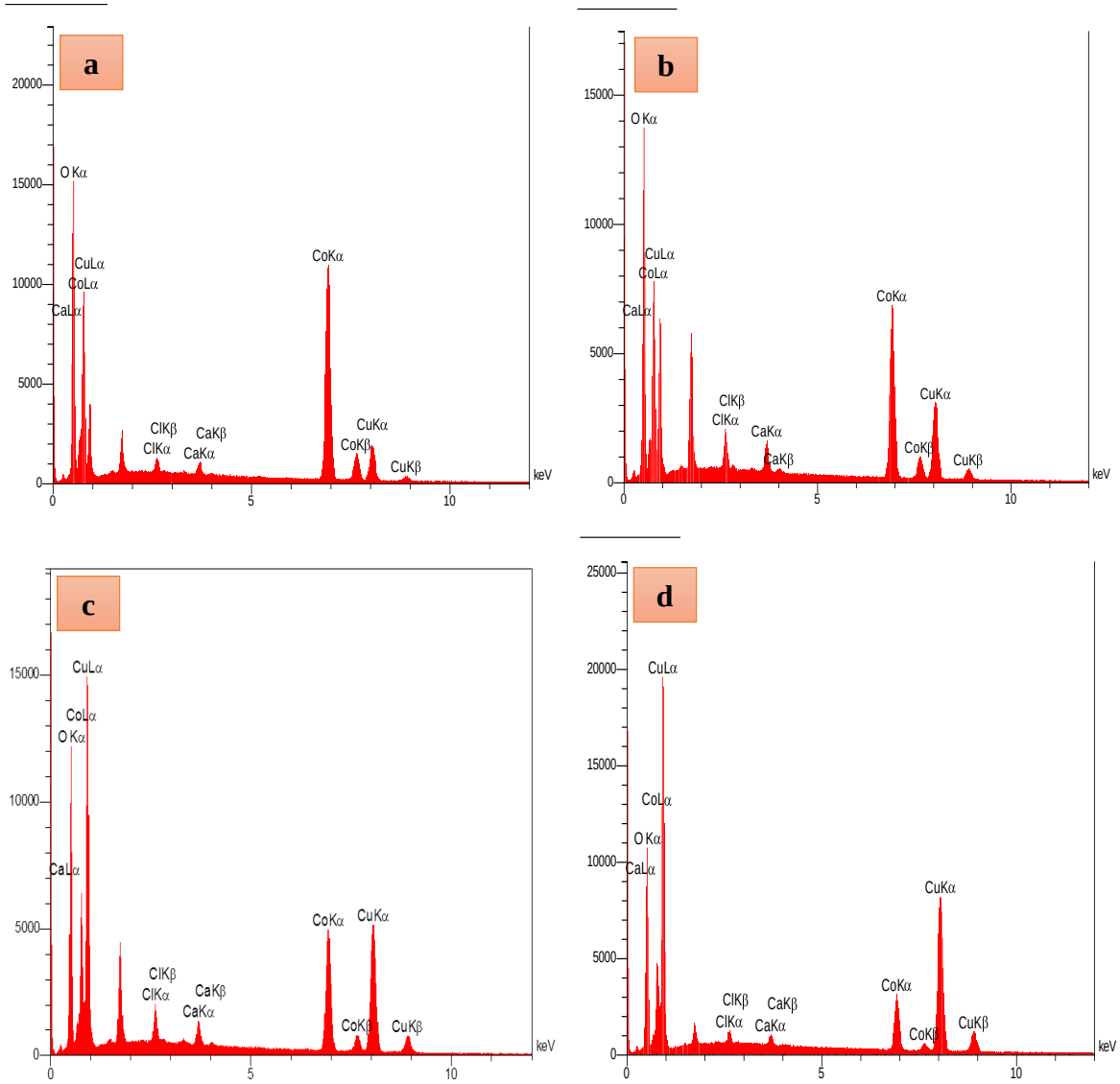

Figure 9: EDS of (a)80% Co_3O_4: 20%CuO (b) 60% Co_3O_4: 40%CuO (c) 40% Co_3O_4: 60%CuO (d) 20% Co_3O_4: 80%CuO thin films.

Table 5: The elements Co, O and Cu in Co_3O_4: CuO samples.

80%Co_3O_4:20%CuO		
Element	W%	A%
O	40.23	70.09
Ca	3.05	2.12
Co	44.06	20.84
Cl	4.03	3.16
Cu	8.63	3.79

60%Co_3O_4:40%CuO		
Element	W%	A%
O	44.11	72.57
Ca	4.81	3.16
Co	28.87	12.89
Cl	6.62	4.92
Cu	15.59	6.46
40%Co_3O_4:60%CuO		
Element	W%	A%
O	41.69	71.01
Ca	4.31	2.93
Co	20.51	9.48
Cl	6.51	5.01
Cu	26.98	11.57
20%Co_3O_4:80%CuO		
Element	W%	A%
O	37.25	68.17
Ca	3.24	2.36
Co	11.40	5.66
Cl	4.47	3.70
Cu	43.64	20.11

4.3 Optical Properties of Co_3O_4: CuO

The absorbance spectrum shows wavelength dependence, with measurements between 300 and 800 nm. Figure 10 illustrates the relationship between absorbance (A) and wavelength for Co_3O_4 thin films mixed with varying percentages of CuO (20%, 40%, 60%, and 80%). As the wavelength increases (corresponding to lower photon energies), the absorbance decreases, aligning with the energy gap of the films. This behavior occurs when the energy of the incoming photon is equal to or less than the energy gap. When the photon energy exceeds the energy gap, it excites electrons, promoting them from the valence band to the conduction band. From the figure, it is evident that the absorbance increases as the CuO content rises. The Tauc plot, which shows the relationship between $(\alpha h\nu)^2$ and $h\nu$ (in eV), allows for the determination of the direct band gap by extrapolating the straight line to $(\alpha h\nu)^2 = 0$, as shown in Figure 11. As summarized in Table 6, the band gap value decreases with increased CuO content. This reduction in the energy gap is attributed to introducing copper oxide levels within the band gap. As the CuO ratio increases, the width of these levels expands, narrowing the overall band gap. These findings are consistent with the results of previous studies [20].

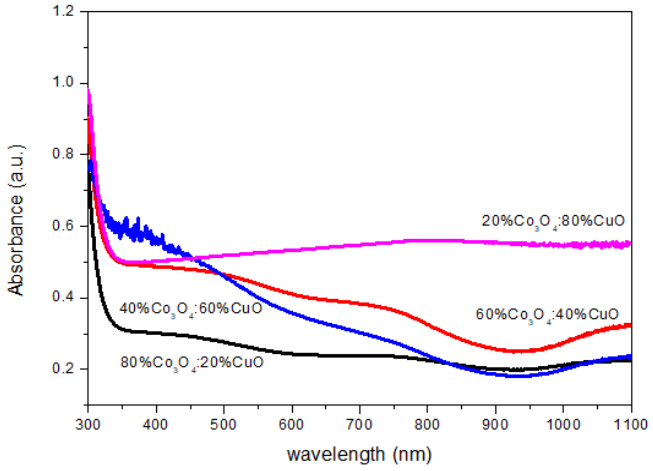

Figure 10: Absorbance of Co_3O_4 mixed with (20, 40, 60 and 80 %) CuO Thin Films.

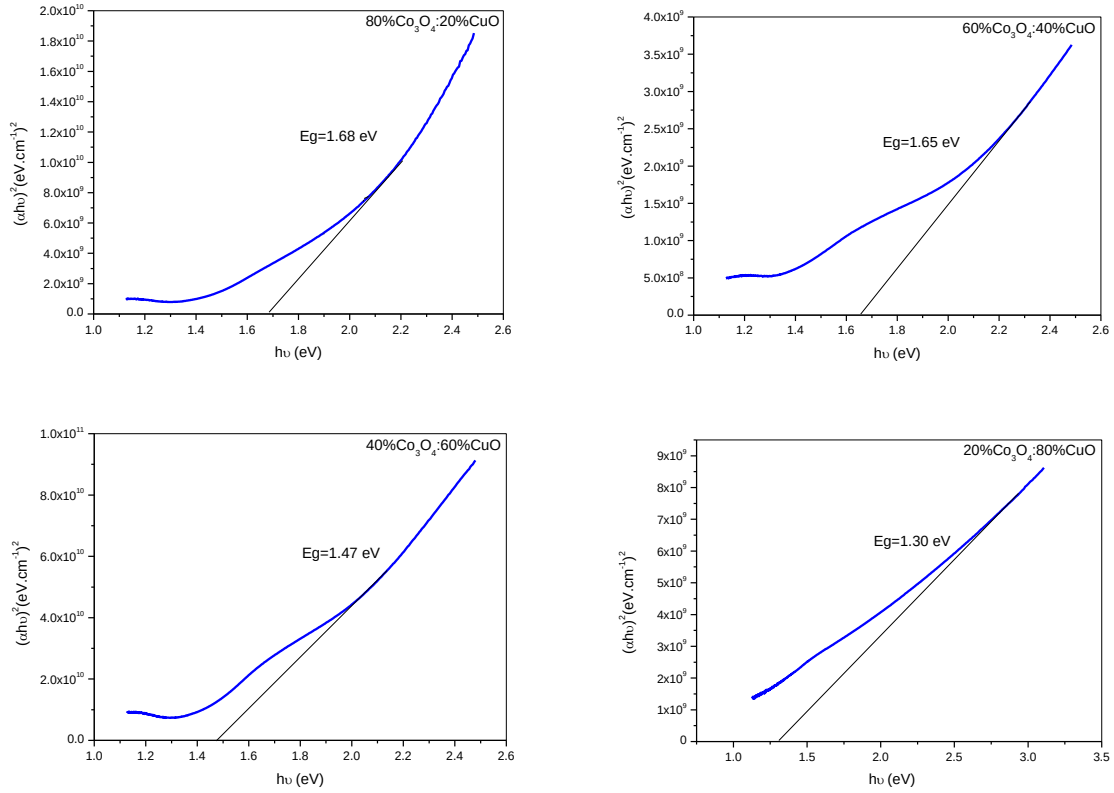

Figure 11: Optical energy band gap of Co_3O_4 mixed with (20, 40, 60 and 80 %)CuO thin films.

Table 6: Energy gap for Co_3O_4 mixed with (20, 40, 60 and 80 %)CuO thin films.

Sample	80%Co_3O_4:20%CuO	60%Co_3O_4:40%CuO	40%Co_3O_4:60%CuO	20%Co_3O_4:80%CuO
E.g. eV	1.68	1.65	1.47	1.30

4.4 Photoluminescence Measurements of Co_3O_4: CuO

The photoluminescence (PL) spectra of Co_3O_4 mixed with 20%, 40%, 60%, and 80% CuO thin films are presented in Figure 12. The primary peak in the PL spectra corresponds to excitonic emissions, which are observed within the wavelength range of 500 to 900 nm. The sample with 80% Co_3O_4: 20% CuO exhibits a strong peak at 575 nm (2.156 eV), followed by 60% Co_3O_4: 40% CuO at 543 nm (2.283 eV), 40% Co_3O_4: 60% CuO at 585 nm (2.119 eV), and 20% Co_3O_4: 80% CuO at 572 nm (2.167 eV). The energy band gap derived from the UV-Vis spectrum is roughly consistent with the location of the peak. Two bands were detected, one at 500 nm and another at 800 nm. The observed changes in absorption and emission properties, along with the slight variation in the nanoparticle band gaps, may be attributed to contaminants, which introduce localized states that affect the optical characteristics [21].

4.5 Hall Effect

Table 7 presents the Hall effect results for cobalt oxide films mixed with 20% and 40% CuO after annealing. The data show that the electrical conductivity of the 80% Co_3O_4: 20% CuO film is higher than that of the 60% Co_3O_4: 40% CuO film, with both exhibiting p-type conductivity. The conductivity of mixed Co_3O_4-CuO were increased significantly compared to pure Co_3O_4 annealed at 500 ^{O}C [22].

5 Conclusions

Thin films of Co_3O_4 mixed with CuO in various ratios were successfully prepared using the chemical spray pyrolysis method. X-ray diffraction analysis revealed that the crystallite size of the films increased with a higher CuO mixing ratio. Surface Morphology (FE-SEM) micrographs showed that higher CuO ratios enhance grain size and promote a denser and more homogeneous surface. However, intermediate CuO ratios (e.g., 40%) displayed some defects, such as cracks and irregular growth patterns, indicating a non-linear the surface morphology evolution with CuO composition. Additionally, the particle size of the films also grew as the CuO content increased. UV

measurements showed the highest absorbance for the 20% Co_3O_4: 80% CuO thin film, while the energy band gap decreased as the CuO ratio increased. The increase in CuO content also resulted in higher absorbance, making the films suitable for optoelectronic applications like solar cells. Electrical conductivity was higher in the 80% Co_3O_4: 20% CuO film compared to the 60% Co_3O_4: 40% CuO film, with all films exhibiting p-type conductivity. The variation in the Co_3O_4-CuO mixing ratio led to tunable band gaps, which could be useful for various technological applications. These findings establish that the physical properties of Co_3O_4:CuO thin films can be effectively tailored by varying the CuO content, making them promising candidates for applications in photovoltaics, sensors, and energy storage devices. Future work could focus on optimizing the deposition parameters, investigating the effects of additional doping, and exploring other post-processing techniques such as laser annealing, in order to enhancing the films' performance.

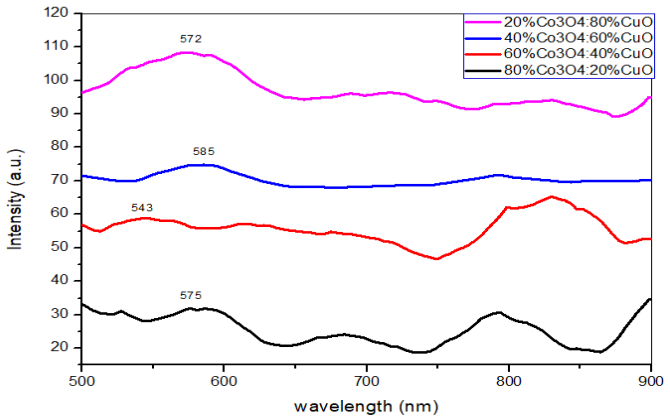

Figure 12: PL of Co_3O_4 mixed with (20, 40, 60 and 80 %) CuO thin films.

Table7: Hall effect for Co_3O_4 mixed with (20 and 40 %) CuO Thin Films.

Sample	n $(cm)^{-3}$	RH $(cm^{-3}C^{-1})$	O. $(\Omega.cm)^{-1}$	μ $(cm^2V^{-1}s^{-1})$	Type
80%Co_3O_4:20%CuO	$7.19x10^{16}$	$8.68x10^{1}$	$2.52\ x10^{1}$	$2.19\ x10^{3}$	P
60%Co_3O_4:40%CuO	$8.07x10^{16}$	$7.73x10^{1}$	$2.24\ x10^{1}$	$1.73\ x10^{3}$	P

References

[1] Barrera, E., Huerta, L., Muhl, S., & Avila, A. Synthesis of black cobalt and tin oxide films by the sol–gel process: surface and optical properties. *Sol. energy mater. Sol. Cells*, **88(2)**, 179-186. (2005).

[2] Xia, X. H., Tu, J. P., Zhang, J., Huang, X. H., Wang, X. L., Zhang, W. K., & Huang, H. Enhanced electrochromics of nanoporous cobalt oxide thin film prepared by a facile chemical bath deposition. *Electrochem. Commun.*, **10(11)**, 1815-1818. (2008).

[3] Shaju, K. M., Jiao, F., Débart, A., & Bruce, P. G. Mesoporous and nanowire Co $_3$ O $_4$ as negative electrodes for rechargeable lithium batteries. *Phys. Chem. Chem. Phys.*, **9(15)**, 1837-1842. (2007).

[4] Yuan, Z., Chen, H., Li, C., Huang, L., Fu, X., Zhao, D., & Tang, J. Facile method to prepare stable superhydrophobic Co_3O_4 surface. *Appl. Surf. Sci.*, **255(23)**, 9493-9497. (2009).

[5] Louardi, A., Rmili, A., Chtouki, T., Elidrissi, B., Erguig, H., Bachiri, A. E., ... & Mejbri, H. Effect of annealing treatment on Co_3O_4 thin films properties prepared by spray pyrolysis. *J. Mater. Environ. Sci*, ***8***, 485-493. (2017).

[6] Klepper, K. B., Nilsen, O., & Fjellvåg, H. Epitaxial growth of cobalt oxide by atomic layer deposition. *J. cryst. Growth*, **307(2)**, 457-465. (2007).

[7] Bahlawane, N., Rivera, E. F., Kohse-Höinghaus, K., Brechling, A., & Kleineberg, U. Characterization and tests of planar Co3O4 model catalysts prepared by chemical vapor deposition. *Appl. Catal. B: Environ.*, **53(4)**, 245-255. (2004).

[8] Švegl, F., Orel, B., Grabec-Švegl, I., & Kaučič, V. Characterization of spinel Co3O4 and Li-doped Co3O4 thin film electrocatalysts prepared by the sol–gel route. *Electrochim. Acta*, **45(25-26)**, 4359-4371. (2000).

[9] Pal, J., & Chauhan, P. Study of physical properties of cobalt oxide (Co_3O_4) nanocrystals. *Mater. Charact.*, **61(5)**, 575-579. (2010).

[10] Chou, S. L., Wang, J. Z., Liu, H. K., & Dou, S. X. Electrochemical deposition of porous Co3O4 nanostructured thin film for lithium-ion battery. *J. Power Sources*, **182(1)**, 359-364. (2008).

[11] Fu, Z. W., Wang, Y., Zhang, Y., & Qin, Q. Z. Electrochemical reaction of nanocrystalline Co3O4 thin film with lithium. *Solid State Ionics*, **170(1-2)**, 105-109. (2004).

[12] Kadam, L. D., Pawar, S. H., & Patil, P. S. Studies on ionic intercalation properties of cobalt oxide thin films prepared by spray pyrolysis technique. *Mater. Chem. and phys.*, **68(1-3)**, 280-282. (2001).

[13] Louardi, A., Rmili, A., Ouachtari, F., Bouaoud, A., Elidrissi, B., & Erguig, H. Characterization of cobalt oxide thin films prepared by a facile spray pyrolysis technique using perfume atomizer. *J. Alloys Compd.*, **509(37)**, 9183-9189. (2011).

[14] Ungeheuer, K., Marszalek, K. W., Mitura-Nowak, M., Perzanowski, M., Jelen, P., Marszalek, M., & Sitarz, M. Influence of Cr ion implantation on physical properties of CuO thin films. *Int. J. of Mol. Sci.*, **23(9)**, 4541. (2022).

[15] Vijitha, S. J., Mohanraj, K., & Jebin, R. P. Structural, optical, and surface modifications by varying precursor concentrations on spray deposition of in doped Co_3O_4 thin films for electro chemical application. *Chem. Phys. Impact*, **6**, 100143. (2023).

[16] Eze, F. C. Electroless deposition of CoO thin films. *J. Phys. D: Appl. Phys.*, **32(5)**, 533. (1999).

[17] Haneen F. Abd, & Ziad T. Khodair. Annealing Effect on Structural and Optical Properties of 〖Cd〗_ (0.91) 〖Ni〗_ (0.09) o Thin Films Prepared by Chemical Spray Pyrolysis. *Academic Science Journal*, **2(4)**, 293–306. (2024).

[18] Abass, A. K., & Abd Al-Hassan, S. A. Effect the Composition Ratio of Cobalt Oxide on the Structural and Optical Properties of Tin Oxide. *Al-Qadisiyah J. Pure Sci.*, **24(3)**. (2019).

[19] Mohammed, N. T., Mansour, J. M., & Aadim, K. A. Structural, Optical and Electrical Properties of (PbS: Co) Nanostructured Thin Films Synthesized by Pulsed Laser Ablation Deposition Technique. *Academic Science Journal*, **1(1)**, 13-28. (2023).

[20] Gassoumi, A., Alleg, S., & Kamoun-Turki, N. Influencing the structural, microstructural and optical properties of PbS nanocrystalline thin films by Mg^{2+} doping. *J. mol. Struct.*, **1116**, 67-71. (2016).

[21] Gopinath, S., Sivakumar, K., Karthikeyen, B., Ragupathi, C., & Sundaram, R. Structural, morphological, optical and magnetic properties of Co3O4 nanoparticles prepared by conventional method. *Physica E: Low-Dimens. Syst. Nanostruct.*, **81**, 66-70. (2016).

[22] Patil, V., Joshi, P., Chougule, M., & Sen, S. Synthesis and characterization of Co_3O_4 thin film. *SNL*, **2(01)**, 1-7. (2012).